# Water structure and dynamics in phosphate fluorosurfactant based reverse micelle: A computer simulation study

Sanjib Senapati and Max L. Berkowitz

Citation: The Journal of Chemical Physics **118**, 1937 (2003); doi: 10.1063/1.1531585
View online: http://dx.doi.org/10.1063/1.1531585
View Table of Contents: http://scitation.aip.org/content/aip/journal/jcp/118/4?ver=pdfcov
Published by the AIP Publishing

# Water structure and dynamics in phosphate fluorosurfactant based reverse micelle: A computer simulation study

Sanjib Senapati and Max L. Berkowitz[a)]
*Department of Chemistry, University of North Carolina at Chapel Hill, Chapel Hill, North Carolina 27599*

(Received 10 September 2002; accepted 29 October 2002)

We performed a molecular dynamics simulation on a system containing a water pool inside the reverse micelle made up of an assembly of phosphate fluorosurfactant molecules dissolved in supercritical carbon dioxide. The water molecules in the first solvation shell of the headgroup lose the water to water tetrahedral hydrogen bonded network but are strongly bonded to the surfactant headgroups. This change in inter-water hydrogen bonding in connection with the confined geometry of the reverse micelle slows down the translational and especially the rotational dynamics of water.
 [DOI: 10.1063/1.1531585]

## I. INTRODUCTION

The behavior of water inside reverse micelles (RM) has been the subject of intense research over the past several years. Thermodynamic and spectroscopic properties of water in reverse micellar systems have been studied using a large variety of experimental techniques, e.g., flourescence probe measurements,[1,2] IR and Raman spectroscopy,[3,4] NMR,[5,6] ESR,[5] and DSC measurements,[5,7] etc. These experiments revealed that in a water-in-oil (w/o) droplet three types of water molecules exist: (i) water molecules bound to the headgroups at the oil–water interface; (ii) free water molecules, that can exchange their state with bound water; and (iii) bulk water. Picosecond emission spectroscopy,[8] fluorescence spectroscopy,[9–11] dielectric measurements,[12,13] femtosecond resolution,[14] and pulsed NMR studies[15] of a water pool confined in reverse micelles and/or in biomolecules have indicated a dramatic slowing down of the rate of relaxation of water molecules. In spite of all these efforts, a good understanding of the nature of water enclosed by the RM is still not achieved.[9,16]

With the recent increase in computing power, computer simulation methods have been employed to study the nature of a RM. Perhaps the first attempt to study a RM using molecular dynamics (MD) simulation was made by Brown and Clarke,[17] who studied water containing RM in an apolar solvent. The micelle in their simulation contained 36 surfactant molecules and a water pool of 72 molecules. The study showed that surfactants formed a coat with a substantial roughness at the aqueous interface and that a considerable number of water molecules penetrated the headgroup surface. However, Brown and Clarke used a highly simplified model in which the surfactant molecules were described by two spherical interaction centers, with one sphere describing the hydrocarbon tails and the other sphere describing the entire headgroup. Thus, specific interactions between water and the sites on the headgroups, which may play a crucial role in water behavior, particularly for those water molecules that are in the first solvation shell of the headgroups, were not taken into account in this study. Linse has examined an AOT-like reverse micellar system.[18] His study indicated that there exists a greater degree of spatial and orientational order of water in the pool, in good agreement with the experimental studies. However, in the study by Linse, the surface of the micelle were assumed to be rigid, which is somewhat unrealistic. Tobias and Klein[19] have investigated the microscopic properties of a calcium carbonate/calcium sulfonate reverse micellar aggregate in nonpolar solvents. They concluded that the structure of the micelle is independent of the solvent and, on average, the water molecules were tightly bound to the surface of the micelle. They, however, did not elaborate on the properties of water in this study. An extensive and careful molecular dynamics simulation study of the water pool in the interior of a reverse micelle was done by Faeder and Ladanyi[20] recently. They found that water forms well-defined layers in the vicinity of the headgroups, where water mobility was greatly reduced. In a separate article the same authors also investigated the solvation dynamics in RM of varying size.[21] The drawback of the work by Faeder and Ladanyi is that they modeled the interior of the RM as a rigid spherical cavity, which again is somewhat unrealistic. Very recently, Salaniwal *et al.* performed molecular dynamics simulations on water/dichain surfactant/carbon dioxide system and demonstrated the self-assembly of reverse micelles.[22] They also studied the structural properties and the kinetics of aggregation of such micelles.[23] Their simulations used realistic molecular models for the components present in the systems. Their results demonstrated a significant penetration of water into the hydrophobic region. However, their interest mostly lay in the study of the structure and kinetics of aggregation, rather than in the exploration of the nature of water in the aqueous core. Clearly, computer simulation studies of water in reverse micelles need to be extended.

In our preceding paper[24] (paper 1), we reported the structure of a reverse micellar aggregate composed of phosphate fluorosurfactant $(C_6F_{13}–(CH_2)_2–O)(C_6F_{13}–(CH_2)_2–O)PO_2^-Na^+$, water and supercritical carbon dioxide. By a combination of molecular dynamics simulation and SANS experiments, we have estimated the size and shape of the

a)Electronic mail: maxb@unc.edu

 

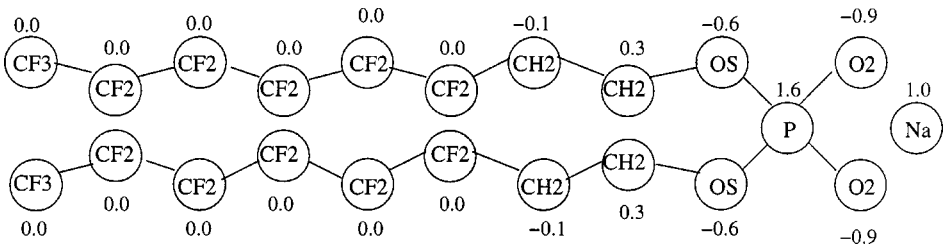


FIG. 1. Structure of the fluorosurfactant molecule. The numbers are the values of the atom-centered point charges.

RM. Since we intended to perform a realistic simulation of a RM, we used a detailed molecular level description of all the species. The description of the potential models was reported in paper 1. The results in paper 1 implied that the RM remained stable over the 4 ns time period of the simulation and the simulation data complemented the SANS experimental results. The radius of gyration of the aqueous core obtained from the simulation was $24.3 \pm 2$ Å. The area per surfactant headgroup was calculated to be $\approx 64$ Å$^2$. The calculated value of micelle eccentricity implied that the RM in our simulation was not a perfectly spherical object. The direct observation of micelle shape fluctuations and the time behavior of eccentricity indicated the stability of the micelle shape on the time scale of the simulation. The results also implied that about 90% of the sodium counterions form contact-ion-pairs with the headgroup atoms and that the interfacial water molecules penetrated the headgroup surface.

To complete our study, we have investigated the structure and dynamics of water in aqueous core of the RM described in paper 1. The results of this work are presented below.

## II. THE MODEL AND SIMULATION DETAILS

We performed a detailed molecular dynamics simulation of an aqueous reverse micelle containing phosphate based fluorosurfactants in supercritical carbon dioxide. Specific details of the model and the procedures used to build the reverse micelle have already been presented in paper 1. The SPC/E model[25] was chosen to describe the water molecules. The SPC/E model is a well-tested and widely used model for liquid water, which has been shown to give a good description of liquid water at both room and supercritical conditions. A single site united atom model was used for $CO_2$.[26] The tails of the surfactant molecules were modeled using the united atom formalism, in which $CH_2$, $CF_2$, and $CF_3$ groups are each replaced by one interaction site centered on the C atom. Every atom in the headgroup was described explicitly. The atom-centered point charges on the surfactant molecules were determined from quantum calculations at the Hartree–Fock level using a GAUSSIAN 98 package[27] with the 6-31+G* basis set. The partial charges along with the structure of the surfactant molecule are shown in Fig. 1. The torsional angle potential for the fluorinated tails of the surfactant molecules were described by a model proposed by Cui *et al.*,[28] and the corresponding parameters are tabulated in Table I. The other interaction parameters used in the calculation are also included in Table I. The torsional potential parameters for the dihedral $CF_2-CH_2-CH_2-OS$ were obtained by performing quantum calculations as described in paper 1. The OPLS parameters[29] were used for the rest of the intermolecular and intramolecular interactions present in the surfactant. The standard combination rules were adopted to obtain the Lennard-Jones parameters for interactions between the different species. All bond lengths were held fixed by applying the SHAKE algorithm[30] with a preset tolerance of $10^{-8}$ Å. This allowed us to integrate the equations of motion with a time step of 2 fs.

TABLE I. Force field parameters for the various species present in the system.[a]

(a) Bond parameters

| Bond | $r_{eq}$ (Å) | Bond | $r_{eq}$ (Å) | Bond | $r_{eq}$ (Å) | Bond | $r_{eq}$ (Å) |
|---|---|---|---|---|---|---|---|
| O2–P | 1.48 | OS–P | 1.61 | $OS-CH_2$ | 1.43 | $CH_2-CH_2$ | 1.54 |
| $CH_2-CF_2$ | 1.54 | $CF_2-CF_2$ | 1.54 | $CF_2-CF_3$ | 1.54 | $O_w-H_w$ | 1.00 |

(b) Angle parameters

| Angle | $k_\theta$ [kcal/(mol rad$^2$)] | $\theta$ (°) |
|---|---|---|
| O2–P–O2 | 280.0 | 119.90 |
| O2–P–OS | 200.0 | 108.20 |
| $P-OS-CH_2$ | 200.0 | 120.50 |
| $OS-CH_2-CH_2$ | 160.0 | 109.50 |
| OS–P–OS | 90.0 | 102.60 |
| $CH_2-CH_2-CF_2$ | 124.14 | 114.0 |
| $CH_2-CF_2-CF_2$ | 124.14 | 114.6 |
| $CF_2-CF_2-CF_2$ | 124.14 | 114.6 |
| $CF_2-CF_2-CF_3$ | 124.14 | 114.6 |
| $H_w-O_w-H_w$ | ··· | 109.4 |

(c) Torsional parameters

| Dihedral | $V_n/2$ (kcal/mol) | $\gamma$(°) | $n$ |
|---|---|---|---|
| $O2-P-OS-CH_2$ | 0.25 | 0.0 | 3 |
| $P-OS-CH_2-CH_2$ | 1.45 | 0.0 | 3 |
| $OS-CH_2-CH_2-CF_2$ | 2.732 | 0.0 | 3 |
| | −1.099 | 30.0 | 1 |
| $OS-P-OS-CH_2$ | 0.25 | 0.0 | 3 |
| | 1.1 | 0.0 | 2 |

(d) Torsional parameters for the surfactant tails $[U(\phi) = a_0 + \Sigma_{i=1}^{7} a_i (\cos\phi)^i$ (Refs. 22, 28)]

| | | | |
|---|---|---|---|
| $a_0 = 959.4$ K | $a_1 = -282.7$ K | $a_2 = 1355.2$ K | $a_3 = 6800.0$ K |
| $a_4 = -7875.3$ K | $a_5 = -14168.0$ K | $a_6 = 9213.7$ K | $a_7 = 4123.7$ K |

(e) van der Waals parameters

| Atom type | $\sigma$ (Å) | $\epsilon$ (kcal/mol) | Atom type | $\sigma$ (Å) | $\epsilon$ (kcal/mol) |
|---|---|---|---|---|---|
| O2 | 2.9578 | 0.210 | P | 3.7418 | 0.200 |
| OS | 2.9934 | 0.170 | $CH_2$ | 3.9300 | 0.09335 |
| $CF_2$ | 4.6000 | 0.05959 | $CF_3$ | 4.6000 | 0.15691 |
| Na | 2.2750 | 0.11522 | $O_w$ | 3.1655 | 0.15539 |
| $H_w$ | 0.0000 | 0.00000 | $CO_2$ | 3.7200 | 0.46895 |

[a]In Tables I(a), I(b), and I(e) $w$ stands for water.

A system containing 1616 water molecules, 160 surfactant molecules, and 6991 $CO_2$ molecules was simulated in a cubic box at 35 °C and 414 bar pressure. To enable volume variation, the simulation was performed in the NPT ensemble, using the Nose–Hoover thermostat and barostat.[31] Both the thermostat and barostat relaxation times were set to 0.5 ps. An equlibration simulation of 200 ps was performed before a production run of 4 ns. Periodic boundary conditions were employed in all directions. The calculation of the long-range Coulombic forces was performed using the smooth particle mesh Ewald (SPME) method.[32] The real space part of the Ewald sum and Lennard-Jones interactions was cut off at 9 Å. We have also simulated a system containing pure bulk water, so that the behavior of water in the confined system can be compared with that of the bulk under the same pressure and temperature. For bulk water, the simulation was carried out in a cubic box containing 512 particles at $T=35\,^{\circ}\mathrm{C}$ and at pressure $P=414$ bar. For the bulk system, periodic boundary conditions were applied in all three directions, minimum image convention was used for the short-range interactions, and the SPME method was employed for the long-range interactions. The bulk water system was equilibrated for 200 ps, and then the production run was continued for 1 ns. Both simulations were carried out using the DLPOLY[33] molecular dynamics simulation package.

## III. RESULTS AND DISCUSSION

### A. Water structure

#### *1. Density distribution*

There is an ambiguity in the literature related to water structure in the interior of a reverse micelle. Faeder and Ladanyi[20] in their molecular dynamics simulation of the interior of aqueous reverse micelle identified that water has a layered structure near the interface. No such layering was observed in the simulation of a reverse micelle by Salaniwal *et al.*[22] We have calculated the number density of water as a function of distance from the center of the aqueous core and the result is shown in Fig. 2. As we see from this figure, no layered structure is found while calculating the density with respect to the center of the aqueous core. The number densities in Fig. 2 were calculated by computing the average number of molecules in spherical shells of thickness $\Delta r = 0.2$ Å, located at various distances from the center of the water pool. As it was demonstrated in the study of liquid/liquid interfaces, a more careful consideration of how to calculate local water density is needed in order to understand the structure of water.[34,35] Similar considerations apply in our case. We observed that the surfactant headgroups form a coat with a substantial roughness at the aqueous interface. This means that the water/headgroup interface is not smooth, but very corrugated, and is fluctuating with time. Moreover, the shape of the water pool is not exactly spherical. These factors will smooth out the local density of water if it is calculated in a simple way like it is done for Fig. 2. Instead we should calculate the local density profile with respect to the headgroup surface. When this is done, the density profile displays the presence of layered structure, which is shown in Fig. 3. The local density of water as a function of distance from the "effective" surface formed by the headgroup phosphorous atoms was computed by following an algorithm proposed very recently in our group and it is described elsewhere.[36]

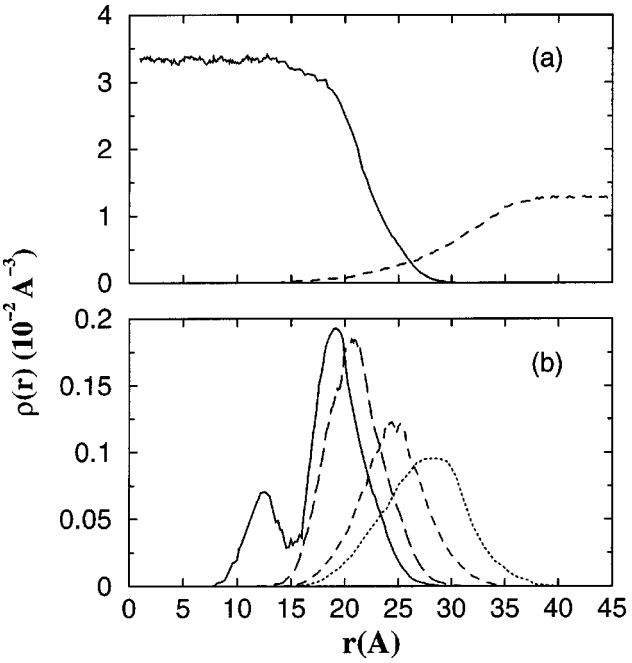


FIG. 2. The number density profile of (a) water (solid line) and carbon dioxide (dashed line) and (b) sodium (solid line), head group phosphorus (long dashed line), tail $CH_2$ (short dashed), and tail $CH_2$ (dotted line) as a function of the distance from the center of the aqueous core.

Figure 2 also indicates that a significant amount of water penetrates the hydrophobic region and essentially hydrates the methylene groups of the surfactant tails. This is possibly due to the electrostatic interactions between water and these groups. The water density then dies down and $CO_2$ molecules take over in the solvation of the surfactant tails. Thus, the surfactant headgroups do not form a rigid surface, rather they create a "soft" surface that water can penetrate to some extent. A similar observation of the penetration of water next to membrane surfaces was reported by our group previously.[37]

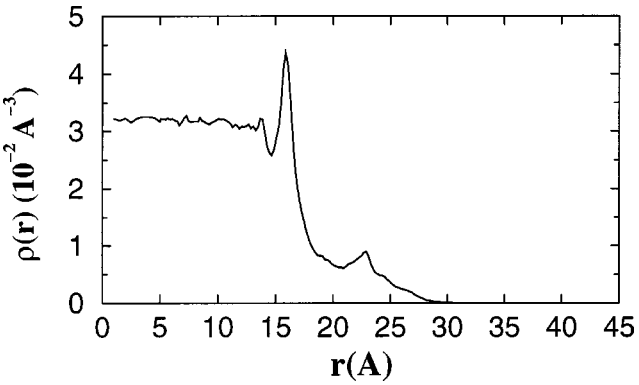


FIG. 3. The number density profile of water with respect to the effective surface formed by the head group phosphorous atoms.

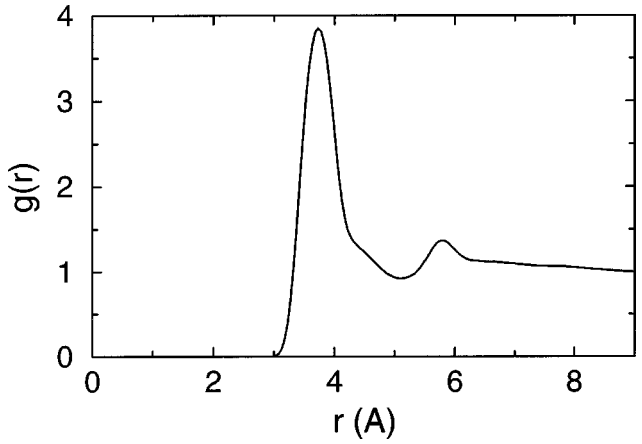


FIG. 4. The pair radial distribution function for $P–O_w$.

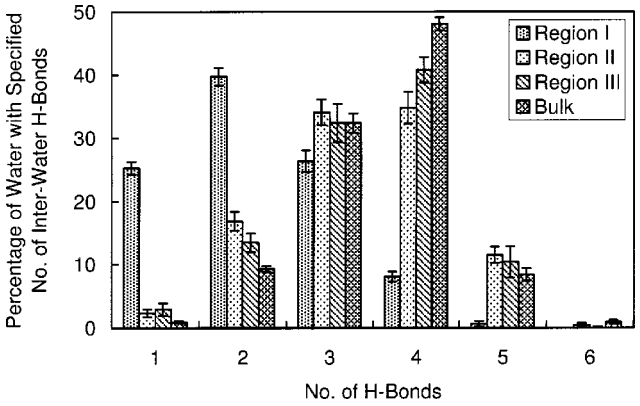


FIG. 5. The distribution of interwater hydrogen bonds for water in the three regions along with the distribution for bulk water. The *x*-axis denotes the number of hydrogen bonds per water molecule and the *y*-axis denotes the percentage of water with that many number of H bonds.

### 2. Hydrogen bond distribution

Exploring properties of confined water is an important field of research. Water in systems like proteins, DNA, and reverse micelles is confined, and this confinement plays a crucial role in the function and stability of these systems. In this study we have investigated the environment and dynamics of confined water in a reverse micelle and the results are shown in Figs. 4–10.

To compare the environment and behavior of water that is in the vicinity of the headgroup surface with water at the center of the aqueous core, we have divided the water pool into three different regions. The size of the first region was selected by a comparison with the size of the first solvation shell observed in the radial distribution function (rdf) for headgroup phosphorus to water oxygen, which is shown in Fig. 4. Thus, region I (or the first shell) consists of water molecules that lie within 5 Å in $P–O_w$ rdf (the distance of first minimum). The rest of the water molecules were assigned to other two regions: region II consisted of molecules between 5–9.5 Å, and region III contained water molecules situated beyond 9.5 Å. The choice of 9.5 Å for the beginning of region III was determined by calculating the hydrogen bond distribution in this region. It was found that the qualitative nature of the water hydrogen bond distribution beyond 9.5 Å matches the distribution in bulk water. The bulk water was simulated at 35 °C and 414 bar pressure.

Albeit water has a very simple molecular structure, it is the tetrahedral hydrogen bonding network that makes it such a complicated but interesting liquid to study. To investigate the water hydrogen bond distribution in various regions of the pool, we adopted a geometric definition of hydrogen bonds.[38] According to this definition, a pair of water molecules is hydrogen bonded if the oxygen–oxygen distance is less than 3.5 Å and simultaneously the oxygen–oxygen–hydrogen angle is less than 30°. Figure 5 shows the distribution of hydrogen bonds (H bonds) between water molecules for the three regions I–III and, for comparison, the distribution for bulk water. The *x* axis on this figure denotes the number of hydrogen bonds per water molecule and the *y* axis denotes the percentage of water with that number of H bonds. As the figure reveals, most of the water molecules in region I lose some of the water-to-water hydrogen bonds. Thus, in region I about 40% of water molecules have two water-to-water H bonds followed by 26% molecules having 3, and 25% having 1 water-to-water H bond. This implies that there exists a strong influence of the head group surface on the water structure at the interface. A rupture in the hydrogen-bonded network is also seen for water in region II, where about 19% of water has 2 water-to-water H bonds and only 33% has 4 water-to-water H bonds. The surface effect diminishes as we move well beyond the surface region and in region III water has hydrogen bond distribution as in the pure bulk water.

The phosphate head groups contain oxygen atoms that are capable of forming hydrogen bonds with first shell water hydrogens. We have studied this capability by computing water–head group hydrogen bonds and the results are shown in Fig. 6. To describe a water–head group hydrogen bond we have used the same geometric definition of hydrogen bonds as for water–water, i.e., a head group and a water molecule are hydrogen bonded if a head group oxygen–water oxygen distance is no greater than 3.5 Å and, simultaneously, the head group oxygen–water oxygen–water hydrogen angle is no greater than 30°. Figure 6 shows that about 40% of water molecules in the first solvation shell of the head groups have one micelle to water H bond, whereas more than 50% of

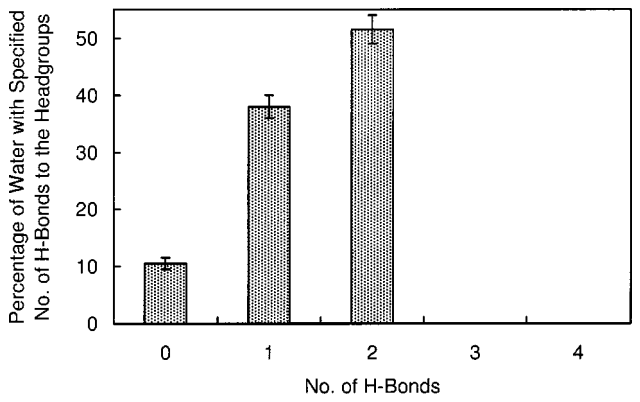


FIG. 6. The distribution of water-to-head group hydrogen bonds. The *y* axis denotes the percentage of water with a specified number of hydrogen bonds to the head groups.

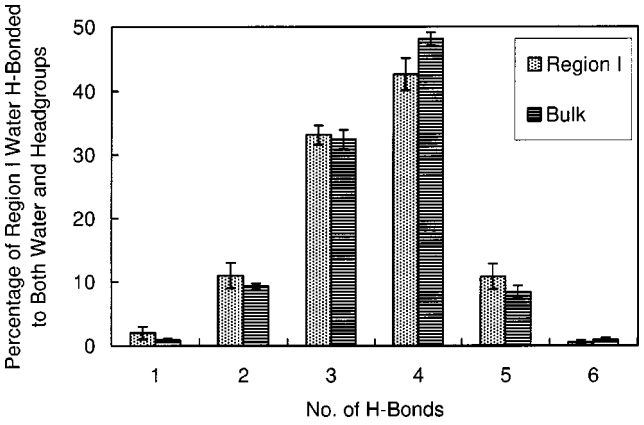


FIG. 7. The hydrogen bond distribution for first shell water molecules taking into account both the interwater and water-to-head group hydrogen bonds. The distribution for bulk water is also included for comparison.

them have 2 micelle to water H bonds. This means that the water molecules in the first solvation shell that lose the tetrahedral hydrogen bonded network try to regain it by forming hydrogen bonds with the headgroup oxygens. To give a quantitative proof of this statement, we computed the hydrogen bond distribution for first shell water molecules, taking into account the formation of hydrogen bonds to both water and micelle head groups. The results are plotted in Fig. 7, which shows the percentage of first shell water hydrogen bonded to both other water molecules and head groups as a function of number of hydrogen bonds per water molecule. Thus Fig. 7 indicates that while considering the hydrogen bond with both the water and micelle, most of the first shell water molecules have four hydrogen bonds followed by three and this closely resembles the hydrogen bond distribution in bulk water.

As we can see, water molecules in the first shell are strongly influenced by the presence of the head group. As we move to the next section, we will find that this structural reorganization of water close to the surface strongly manifests itself in the dynamics, and the mobility of water molecules in shell I is reduced significantly. Therefore we specify these water in region I as "bound water." The head group surface influences water molecules in region II also, but the effect is not that significant and, as we shall see, water molecules in this region are more mobile compared to water in region I. We, therefore, designate these water molecules as "free or diffuse water." Water molecules in region III are very slightly affected by the surface and essentially behave like bulk water. We call them "bulklike water."

## B. Water dynamics

A variety of experiments demonstrated that water in confined environments next to proteins, micelles, and in the pools of reverse micelles displays a slow component in the reorientational dynamics or in its response to perturbation in solute properties. Thus, dielectric relaxation,[13,39] solvation dynamics,[8–10] NMR relaxation dispersion,[39] etc. measurements have shown that this slow component decays in hundreds to thousands of picoseconds. In a recent article on ultrafast dynamics in reverse micelles,[9] Levinger has concluded that the slow components are always present in the dynamics of water in restricted environments, and the source of these slow relaxation components may be discussed in terms of solvent bound to the molecular assembly, and to the immobilization of the solvent in a confined environment. Very recently, Bagchi and co-workers[40] have reported that the dramatic slowing down of water reorientational dynamics can be explained partly due to the formation of hydrogen bonds between water and surface head groups. By a detailed molecular dynamics simulation study they have shown that the decay of the reorientational motion of water molecules near the micellar surface is slower than the one in bulk water by two orders of magnitude. In a very recent simulation of a system containing a SDS micelle in water, we also observed the slowing down of the decay in the reorientational correlation function of water next to the micellar surface,[41] thus confirming the analysis of Bagchi and collaborators.

For a further understanding of the origin of this slow decay, we have analyzed the mobility of water in the restricted environment of a reverse micelle. Since our interest is mostly concentrated on the slow dynamics of water we, following the prescription proposed by Bagchi and collaborators, pay attention only to those water molecules that have large residence times in their respective shells. Therefore, while calculating a dynamical quantity, we follow only those water molecules that stay in their respective shells throughout a particular run.[40] We also want to choose a fair number of molecules in every shell so we can obtain a good averaging. One may wonder if this will not restrict our choice substantially, since very few water molecules will qualify for our consideration. Nevertheless, we found that 25 water molecules stayed in region I throughout a time period of 1.8 ns, at least 18 molecules stayed in region II for a time period of 160 ps, and at least 15 molecules stayed in region III throughout a time period of 20 ps (since water molecules are more mobile in regions II and III, they stayed in those regions for shorter time periods). We calculated the translational and reorientation mobilities of these molecules in different regions.

### 1. Translational mobility

A good measure of water translational mobility can be obtained from the time dependence of the mean square displacement (MSD) of water molecules. The diffusion coefficient D can be calculated from the long time behavior of the MSD of water molecules and it is related to the slope of the MSD by the Einstein relation, which in three dimensions reads as

$$D = \lim_{t\to\infty} \frac{\langle |\mathbf{r}(t) - \mathbf{r}(0)|^2 \rangle}{6t}, \tag{1}$$

where $\mathbf{r}(t)$ is the position vector of a water molecule at time $t$. We have computed the MSD for water molecules in all three regions I–III and for the bulk water as a function of time and the results are shown in Fig. 8. From this figure we observe that the diffusion in the first solvation shell is considerably slower than the diffusion in the bulk phase. We have pointed out in the previous section that at least 50% of the first shell water molecules form 2 surfactant to water H

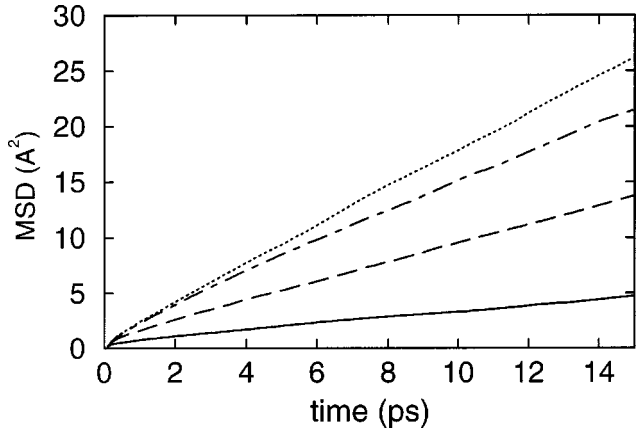


FIG. 8. The time dependence of the mean square displacement for water molecules at various regions along with the bulk water. The solid line is for water molecules who remain in region I continuously for 1.8 ns, the long-dashed line is for water molecules who remain in region II continuously for 160 ps, the dot–dashed line is for water molecules who remain in region III continuously for 20 ps, and the dotted line is for bulk water. All the curves are cut at 15 ps to show clearly the differences between various regions.

bonds and about 40% of them from 1 H bond to the surfactant oxygen. The formation of hydrogen bonds between the head group oxygens and water restricts significantly the translational motion of water in region I. The translational motion of water in region II is also restricted, but the surface effect is not that profound in this region. The water mobility then increases as we move away from the surface and at the center of the aqueous core (region III) it approaches a value that is close to the bulk water mobility. We have calculated the diffusion coefficients for all the three regions and also for the bulk water from a linear fit to the slope of the mean square displacement curves. The values are included in Table II. The data show that the translational mobility for slow water molecules in the first shell is reduced by a factor of 6 compared to bulk water.

### 2. Reorientational dynamics

The reorientational motion of water can be partially characterized by calculating its single dipole autocorrelation function $C_\mu(t)$. Again in our calculations of the dipolar correlation function, we considered only those water molecules that stayed in their corresponding regions for the calculation time. The single dipole autocorrelation function is defined as

$$C_\mu(t)=\langle \mu_i(t)\cdot\mu_i(0)\rangle/\langle \mu_i(0)\cdot\mu_i(0)\rangle, \tag{2}$$

where $\mu_i(t)$ is the dipole vector of the $i$th water molecule at time $t$ and the averaging is performed by water molecules and a time origin. In Fig. 9, we have displayed the relaxation of $C_\mu(t)$ for water molecules in all the three regions and also included the result for bulk water at a specified temperature and pressure. The reorientational motion of water in regions

TABLE II. Values of translational diffusion coefficients at various regions.

| Region | I | II | III | Bulk |
|---|---|---|---|---|
| $D(10^{-9}\ \mathrm{m^2/s})$ | 0.45±0.05 | 1.59±0.13 | 2.21±0.20 | 2.70±0.10 |

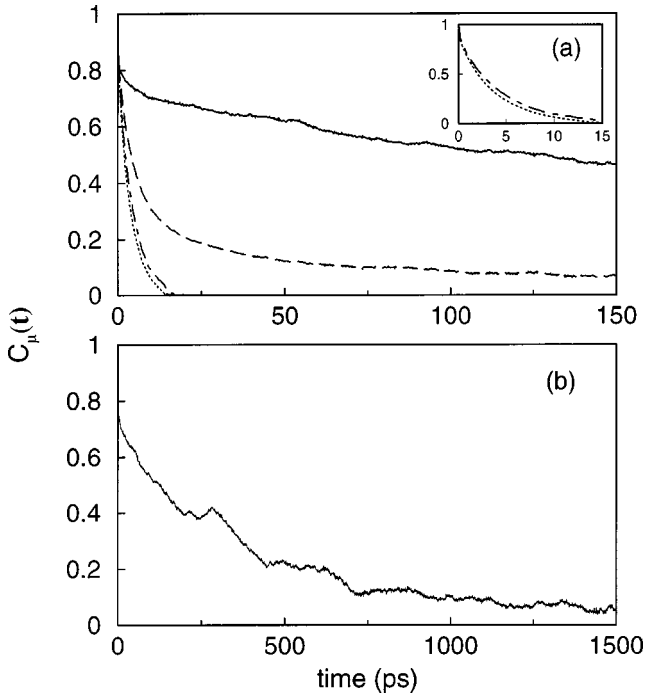


FIG. 9. The time dependence of the single dipole orientational correlation function for water molecules in various regions. The different curves are as in Fig. 8.

I and II is highly nonexponential involving a very slowly decaying tail. A significantly slower decay is observed for the water molecules in region I compared to bulk water. This is quite expected, since as we observed (see Fig. 6) that about 90% of water molecules in the first solvation shell are tightly bound to the head groups. Therefore, these hydrogen bonds between the head group oxygens and the interfacial water molecules restrict the rotational motion of water significantly. A similar and dramatic slowdown in the decay of the water reorientational relaxation was reported by Bagchi and co-workers for water near the micellar surface[40] and by us,[41] also near a micellar surface. To get a quantitative estimate of the reorientational decay time we calculated (a) the average orientational correlation time, $\tau$, for various regions, which is defined by the following equation:

$$\tau=\int_0^\infty dt\, C_\mu(t). \tag{3}$$

Since our correlation function was calculated up to a finite time, to estimate the behavior of this function at longer times, we fitted the dipolar autocorrelation function to a multiexponent function of the following form:

$$C_\mu(t)=\sum_{i=1}^{4} A_i \exp(-t/\tau_i), \tag{4}$$

where $\Sigma_{i=1}^4 A_i=1$ and $\tau_i$ is the time constant for the decay of the $i$th component. Finally, from Eq. (3) and using Eq. (4) for the extrapolation of the long-time tail region, we obtained the following estimates for the values of average orientational correlation times: 396, 41, and 3.8 ps for water molecules in regions I, II, and III, respectively. The corresponding value for bulk water is 3.2 ps. The value of $\tau$ obtained by

Bagchi and co-workers for water near the micellar surface of cesium pentadecafluorooctanoate micelle was 108 ps at 300 K. (b) We calculated the time constants for the long time decay of water molecules in regions I and II from a fit given by Eq. (4). The time constants for the long-time decay were found to be 1700 and 150 ps for water molecules in regions I and II, respectively. This indicates that the slow component of reorientational relaxation of water in the solvation layer is slowed down by three orders of magnitude compared to bulk water, which is in good agreement with the experimental observations on a water pool in reverse micelles.[8,11] We also noticed that the value of the time constant for the long-time decay obtained by Bagchi and co-workers for water near the micellar surface of cesium pentadecafluorooctanoate micelle was 767.1 ps at 300 K. Thus, we observe that water inside our reverse micelle relaxes with a rate that is somewhat slower than the relaxation rate observed for water near a micellar surface. It is, however, worth emphasizing that the average relaxation rates given above are just estimates that depends on the quality of extrapolation and statistics. Nevertheless, previous simulations and the present simulations clearly show that water next to hydrophilic surfaces is substantially slowed down. The quantitative value of this effect depends on the details of the system and also on the state conditions at which the simulations are performed. In Fig. 9(b) we show the dipole autocorrelation function for the 25 water molecules from region I plotted up to 1.5 ns. As we can see, the function still does not decay to zero, indicating that the rotation of water is restricted. The similar behavior of water next to the micellar surface, was also observed by Bagchi and collaborators. The relaxation of $C_\mu(t)$ for water far from the surface (region III) is essentially identical with that of $C_\mu(t)$ in bulk water and is shown in the inset of Fig. 9(a).

To strengthen our notion that the strong water–head group hydrogen bonding is one of the important factors responsible for the dramatic slow decay of the water reorientational relaxation, we performed two more molecular dynamics simulations. In both simulations we froze the motion of the surfactant molecules in the aggregate with, in one case, making them uncharged (and therefore creating a cavity with hydrophobic surface) and in the other case keeping the charges intact. Figure 10(a) shows the decay of $C_\mu(t)$ as a function of time for the slow molecules in region I for all the three systems studied. The correlation functions were calculated for those water molecules that stayed in region I for 150 ps. There were 370 of these molecules when the frozen head groups were charged, 52 when they were uncharged, and we looked at 220 water molecules when the system was in its normal state. As we can see from the figure, the slowest relaxation is observed in the system with the frozen charged groups. This is due to the fact that when we remove the movement of the head group atoms that otherwise are vibrating rapidly, the water molecules get a better hold of head group oxygens to form more stable hydrogen bonds. We also observe that the relaxation of water molecules near the hydrophobic surface is much faster than next to the charged surfaces. This indicates that the water–head group hydrogen bond formation is, perhaps, the most important factor in determining the slow dynamics of water in restricted environments. It is also worth noticing that the relaxation of water molecules near the hydrophobic surface is slower compared to bulk water. This slowing down can be attributed to the confined geometry of the system. Thus, the formation of water–head group hydrogen bonds in connection with the confined geometry of the reverse micelle resulted in a significantly slower water dynamics compared to the dynamics of water in the bulk, which confirms the prediction of Levinger.[9] In Fig. 10(b) the relaxation of slow water molecules in region II is compared for all three systems. As we can see, in region II, where the surface effect is weak, the water molecules in all three systems show almost similar behavior.

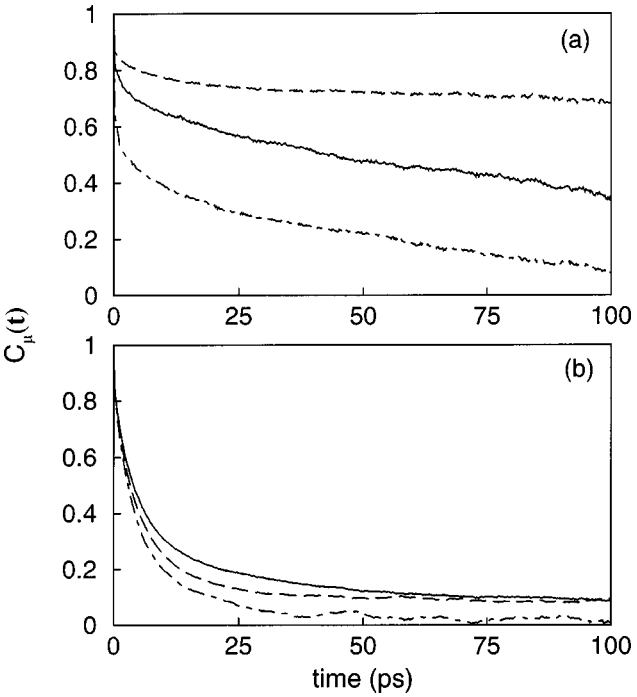


FIG. 10. The time dependence of the single dipole orientational correlation function for water molecules (a) in region I, (b) in region II. The solid line is for water molecules in the original system, the long-dashed line is for water molecules in a system where the motion of the surfactant molecules was frozen, and the dot–dashed line is for water molecules in a hydrophobic cavity with the motion of the surfactant molecules frozen. The correlation functions in each system were calculated by looking at those water molecules that stayed continuously in their respective regions for 150 ps.

## IV. SUMMARY AND CONCLUSIONS

The slowing down in the dynamics of water next to surfaces of molecules such as proteins or molecular assemblies such as micelles and reverse micelles was observed in a number of experiments. It was also observed in a number of molecular dynamics simulations performed on detailed models of micelles or proteins solvated in water. The present simulation confirms that the same slowing down of the water dynamics occurs in the solvation region inside a reversed micelle, thus confirming the experimental observations and previous model studies of this type of system. Our present simulation was performed on a system containing a water pool inside the reverse micelle made up of an assembly of

phosphate fluorosurfactant molecules dissolved in supercritical carbon dioxide. We observed that the slow component of reorientational relaxation of water in the solvation layer is slowed down by three orders of magnitude, in agreement with the experimental results.[8,11] We also observed that the translational dynamics is slowed down, but only by a factor of 6. The structural analysis of water inside the pool shows that water tries to preserve its four coordinated hydrogen bonding network by replacing water to water hydrogen bonds with water to micellar surface hydrogen bonds. Although the distribution of hydrogen bonds for different regions is not changed dramatically, the replacement of water to water flickering hydrogen bonds by more stable water to micelle H bonds substantially slows down the dynamics of water in the solvation shell, especially its rotational dynamics. It is interesting that this substantial slowing down in the dynamics is rather localized and it is mostly gone at a distance of 1 nm away from the surface. The water molecules that are in the region between the solvation layer and bulk-like water serve as a buffer and allow for a gradual change in water properties. A comparison of our simulations and other simulations[40,41] indicate that the substantial slowing down in the water dynamics is a general effect, although the magnitude and details of this effect depend on the specific system.

## ACKNOWLEDGMENTS

This work was supported by the Kenan Center for the Utilization of Carbon Dioxide in Manufacturing and the STC Program of the National Science Foundation under Agreement No. CHE-9876674. The simulations were performed on an IBM SP machine at the North Carolina Supercomputing Center.

[1] M. Belletete, M. Lachapelle, and G. Durocher, J. Phys. Chem. **94**, 5337 (1990).
[2] T. K. De and A. Maitra, Adv. Colloid Interface Sci. **59**, 95 (1995).
[3] A. D'Aprano, A. Lizzio, V. Turco Liveri, F. Aliotta, C. Vasi, and P. Migliardo, J. Phys. Chem. **92**, 4436 (1988).
[4] T. K. Jain, M. Varshney, and A. Maitra, J. Phys. Chem. **93**, 7409 (1989).
[5] H. Hauser, G. Haering, A. Pande, and P. L. Luisi, J. Phys. Chem. **93**, 7869 (1989).
[6] F. Heatley, J. Chem. Soc., Faraday Trans. **85**, 917 (1989).
[7] C. Boned, J. Peyrelasse, and M. Moha-Ouchanne, J. Phys. Chem. **90**, 634 (1986).
[8] N. Sarkar, A. Datta, S. Das, and K. Bhattacharyya, J. Phys. Chem. **100**, 15483 (1996); N. Sarkar, K. Das, A. Datta, S. Das, and K. Bhattacharyya, J. Phys. Chem. **100**, 10523 (1996); S. Das, A. Datta, and K. Bhattacharyya, J. Phys. Chem. A **101**, 3299 (1997); A. Datta, D. Mandal, S. K. Pal, and K. Bhattacharyya, J. Phys. Chem. B **101**, 10221 (1997).
[9] N. E. Levinger, Curr. Opin. Colloid Interface Sci. **5**, 118 (2000).
[10] R. E. Riter, D. M. Willard, and N. E. Levinger, J. Phys. Chem. B **102**, 2705 (1998); R. E. Riter, E. P. Undiks, and N. E. Levinger, J. Am. Chem. Soc. **120**, 6062 (1998); D. Pant, R. E. Riter, and N. E. Levinger, J. Chem. Phys. **109**, 9995 (1998).
[11] J. Zhang and F. V. Bright, J. Phys. Chem. **95**, 7900 (1991).
[12] E. H. Grant, V. E. R. McClean, N. R. V. Nightingale, R. J. Sheppard, and M. J. Chapman, Bioelectromagnetics **7**, 151 (1986).
[13] M. Fukuzaki, N. Miura, N. Sinyashiki, D. Kunita, S. Shiyoya, M. Haida, and S. Mashimo, J. Phys. Chem. **99**, 431 (1995).
[14] S. K. Pal, J. Peon, and A. H. Zewail, Proc. Natl. Acad. Sci. U.S.A. **99**, 1763 (2002).
[15] (a) D. W. Urry, S. Peng, J. Xu, and D. T. McPherson, J. Am. Chem. Soc. **119**, 1161 (1997); (b) P. S. Bolton, J. Phys. Chem. **99**, 17061 (1995).
[16] G. W. Robinson, S. Zhu, S. Singh, and M. W. Evans, *Water in Biology, Chemistry and Physics* (World Scientific, Singapore, 1996).
[17] D. Brown and J. H. R. Clarke, J. Phys. Chem. **92**, 2881 (1988).
[18] P. Linse, J. Chem. Phys. **90**, 4992 (1989).
[19] D. J. Tobias and M. L. Klein, J. Phys. Chem. **100**, 6637 (1996).
[20] J. Faeder and B. M. Ladanyi, J. Phys. Chem. B **104**, 1033 (2000).
[21] J. Faeder and B. M. Ladanyi, J. Phys. Chem. B **105**, 11148 (2001).
[22] S. Salaniwal, S. T. Cui, H. D. Cochran, and P. T. Cummings, Langmuir **17**, 1773 (2001); **15**, 5188 (1999).
[23] S. Salaniwal, S. T. Cui, H. D. Cochran, and P. T. Cummings, Ind. Eng. Chem. Res. **39**, 4543 (2000).
[24] S. Senapati, J. S. Keiper, J. M. DeSimone, G. D. Wignall, Y. B. Melnichenko, H. Frielinghaus, and M. L. Berkowitz, Langmuir **18**, 7371 (2002).
[25] H. J. C. Berendsen, J. R. Grigera, and T. P. Straatsma, J. Phys. Chem. **91**, 6269 (1987).
[26] H. Higashi, Y. Iwai, H. Uchida, and Y. Arai, J. Supercrit. Fluids **13**, 93 (1998).
[27] M. J. Frisch, G. W. Trucks, M. Head-Gordon *et al.*, GAUSSIAN 98, Revision A.6, Gaussian, Inc., Pittsburgh, PA, 1998.
[28] S. T. Cui, J. I. Siepmann, H. D. Cochran, and P. T. Cummings, Fluid Phase Equilib. **146**, 51 (1998).
[29] W. Jorgensen and J. Tirado-Rives, J. Am. Chem. Soc. **110**, 1657 (1988).
[30] G. Cicotti and J. P. Ryckaert, Comput. Phys. Rep. **4**, 345 (1986).
[31] S. Nose, J. Chem. Phys. **81**, 511 (1984); W. G. Hoover, Phys. Rev. A **31**, 1695 (1985).
[32] U. Essmann, L. Perera, M. L. Berkowitz, T. Darden, H. Lee, and L. G. Pedersen, J. Chem. Phys. **103**, 8577 (1995).
[33] W. Smith and T. R. Forester, DLPOLY, 2.12 version; CCLRC; Daresbury Laboratory, 1999.
[34] P. A. Fernandes, M. N. D. S. Cordeiro, and J. A. N. F. Gomes, J. Phys. Chem. B **103**, 8930 (1999).
[35] S. R. P. da Rocha, K. P. Johnston, R. E. Westacott, and P. J. Rossky, J. Phys. Chem. B **105**, 12092 (2001).
[36] S. A. Pandit, D. Bostick, and M. L. Berkowitz, Biophys. J. (to be published).
[37] U. Essmann, L. Perera, and M. L. Berkowitz, Langmuir **11**, 4519 (1995).
[38] A. Luzar and D. Chandler, Phys. Rev. Lett. **76**, 928 (1996); Nature (London) **379**, 53 (1996).
[39] B. Halle, V. P. Denisov, and K. Venu, in *Biological Magnetic Resonance*, edited by N. Ramakrishna and L. J. Berliner (Kluwer Academic/Plenum, New York, 1999), Vol. 17, p. 419.
[40] S. Balasubramanian and B. Bagchi, J. Phys. Chem. B **106**, 3668 (2002); S. Balasubramanian, S. Pal, and B. Bagchi, Curr. Sci. **82**, 845 (2002); S. Pal, S. Balasubramanian, and B. Bagchi, J. Chem. Phys. **117**, 2852 (2002).
[41] C. D. Bruce, S. Senapati, M. L. Berkowitz, L. Perera, and M. D. E. Forbes, J. Phys. Chem. B **106**, 10902 (2002).